PROCEEDINGS OF SPIE

SPIEDigitalLibrary.org/conference-proceedings-of-spie

Photoacoustic differentiation of cortical from cancellous bone in the lumbar vertebrae of an intact human cadaver to prevent bone breaches during spinal fusion surgeries

Gonzalez, Eduardo, Jain, Amit, Lediju Bell, Muyinatu

Eduardo Gonzalez, Amit Jain, Muyinatu A. Lediju Bell, "Photoacoustic differentiation of cortical from cancellous bone in the lumbar vertebrae of an intact human cadaver to prevent bone breaches during spinal fusion surgeries," Proc. SPIE 11642, Photons Plus Ultrasound: Imaging and Sensing 2021, 1164210 (5 March 2021); doi: 10.1117/12.2579025

SPIE.

Event: SPIE BiOS, 2021, Online Only

Downloaded From: https://www.spiedigitallibrary.org/conference-proceedings-of-spie on 28 Mar 2021 Terms of Use: https://www.spiedigitallibrary.org/terms-of-use

Photoacoustic differentiation of cortical from cancellous bone in the lumbar vertebrae of an intact human cadaver to prevent bone breaches during spinal fusion surgeries

Eduardo Gonzalez[a], Amit Jain[b], and Muyinatu A. Lediju Bell[a,c,d]

[a]Department of Biomedical Engineering, Johns Hopkins University, Baltimore, MD, USA
[b]Department Orthopaedic Surgery, Johns Hopkins University, Baltimore, MD,USA
[b]Department of Electrical and Computer Engineering, Johns Hopkins University, Baltimore, MD, USA
[c]Department of Computer Science, Johns Hopkins University, Baltimore, MD, USA

ABSTRACT

In spinal fusion surgeries, it is critical to maintain correct trajectories during the process of creating pedicle holes for screw insertion, in order to avoid accidental bone breaches and screw misplacement, which are characterized by screws placed within surrounding cortical bone rather than the cancellous core of the pedicle. One key difference between these two bone types is the greater porosity of the cancellous bone when compared to the more dense, more compact cortical bone. This work investigates the feasibility of using photoacoustic imaging to differentiate cortical from cancellous bone in the lumbar vertebrae of an intact human cadaver, with the ultimate goal of developing a novel photoacoustic surgical system to prevent breaches. Eleven pedicle cannulations were performed in the lumbar vertebrae of a human cadaver, including six holes in the cancellous core and five partial or complete breaches of surrounding cortical bone. Amplitude-based delay-and-sum (DAS), coherence-based short-lag spatial coherence (SLSC), and locally weighted SLSC (LW-SLSC) beamforming were used to characterize differences in the morphology of photoacoustic signals originating from cancellous and cortical bone. Statistically significant differences between the median of measured areas from cortical and cancellous bone measured 6.61 mm^2 for -6 dB contours obtained with DAS beamforming and ranged from 2.89 mm^2 to 42.13 mm^2 for -10 dB and -15 dB contours obtained with DAS, SLSC, and LW-SLSC beamforming ($p<0.001$). In addition, coherence-based photoacoustic imaging enabled localization of the tip of the optical fiber that was inserted into each prepared pedicle hole. Therefore, both DAS and SLSC beamforming has the potential to synergystically detect the tip of surgical tools and differentiate between signals originating from cortical and cancellous bone. These results are promising for surgical guidance within the desired cancellous core of the pedicle and away from the surrounding cortical bone, in order to avoid costly and painful bone breaches during surgery.

1. INTRODUCTION

Spinal instability can be caused by degenerative disorders, trauma, and primary or metastatic cancer.[1] These abnormalities are commonly treated with spinal fusion surgeries, which help to alleviate pain and recover neurological functionality. Contemporary posterior spinal fusion surgeries involve creating holes in the pedicles of vertebrae, inserting pedicle screws, and attaching each screw to a metal rod with the goal of stabilizing the spine to allow for bony fusion. When cannulating pedicles, it is critical to ensure the correct trajectory during the hole creation process in order to avoid accidental bone breaches and screw misplacement,[2] which compromises neighboring structures of the peripheral and central nervous system, erodes long-term biomechanical stability,[2,3] and causes adjacent degeneration.[4,5] These breaches occur in 14% to 38.5% of procedures, characterized by misplaced screws within the surrounding cortical bone rather than the cancellous core of the pedicle,[6] as shown in Fig. 1.

One key difference between cancellous and cortical bone is the greater porosity of the cancellous bone when compared to the more dense, more compact cortical bone.[8] This difference can be visualized in conventional computer-assisted methods such as computed tomography (CT),[9] 2D-,[10] and 3D-fluoroscopy navigation,[11] where the brightest pixels are indications of high attenuation values originating from cortical bone. However, limitations

Photons Plus Ultrasound: Imaging and Sensing 2021, edited by Alexander A. Oraevsky
Lihong V. Wang, Proc. of SPIE Vol. 11642, 1164210 · © 2021 SPIE
CCC code: 1605-7422/21/$21 · doi: 10.1117/12.2579025

Downloaded From: https://www.spiedigitallibrary.org/conference-proceedings-of-spie on 28 Mar 2021
Terms of Use: https://www.spiedigitallibrary.org/terms-of-use

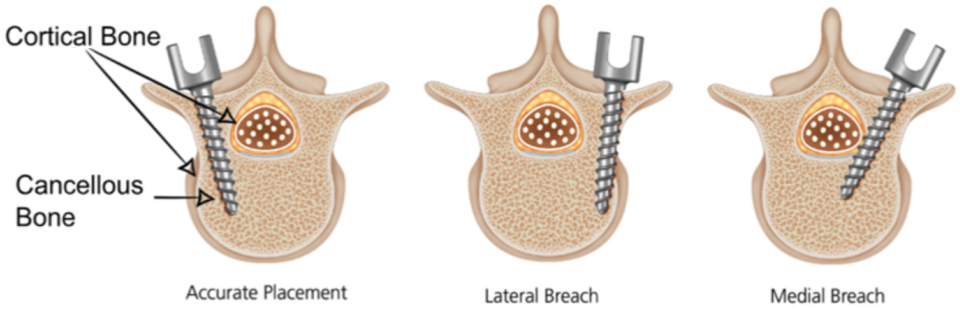

Figure 1: Examples of accurate and inaccurate pedicle screw placement.[7]

of these methods include exposure to ionizing radiation, the requirement to insert reference and intraoperative markers, and relatively prolonged surgery times.

To overcome the limitations listed above, our group recently proposed photoacoustic imaging as a guidance method for pedicle screw insertion.[12,13] The proposed technique consists of delivering laser light at the tip of a device (e.g., pedicle probe, drill) while it is being inserted into the pedicle to create a hole for the screw. The emission of laser pulses generate an acoustic pressure response from the surrounding bone. The acoustic pressure is then received by an externally placed ultrasound probe, and beamforming is applied to create a photoacoustic image. As cancellous bone is more blood-rich in comparison to cortical bone, a distinctive photoacoustic response is expected between these two types of bone. This distinction was demonstrated when visualizing photoacoustic signals from the surface of a human vertebra[12] and when visualizing photoacoustic signals from beneath the bony surface in a more realistic setup and closer to the surgical environment of a spinal fusion surgery.[14]

The work in this paper expands our previous work[14] by providing a more detailed analysis of the ability to distinguish cortical from cancelleous bone when photoacoustic signals originate from beneath the bone surface. This more detailed analysis is performed in the lumbar vertebrae of an intact human cadaver, with the ultimate goal of developing a novel photoacoustic surgical system to prevent breaches. Coherence-based beamforming techniques such as short-lag spatial coherence (SLSC)[15] and locally weighted short-lag spatial coherence (LW-SLSC)[16] were investigated in addition to conventional delay-and-sum (DAS) beamforming to characterize signal morphology as well as to determine the location of the fiber tip that initiates the photoacoustic effect.

2. METHOD

An adult male human cadaver was placed in the prone position and dissection was carried along the cranio-caudal axis with the aid of a Cobb elevator to reveal the spinous process, lamina, and facet joints at each level from L1 to S1. The specimen had no reports of spine pathologies, malformations, or previous spinal surgeries, which was also confirmed with pre-operative CT imaging. The pedicles were cannulated bilaterally from L2 through L4 along anatomic trajectories using a standard free hand technique with a pedicle probe.

Six pre-bored holes were created in the cancellous core of the pedicle, and five pre-bored holes either created an intentional breach of the lateral wall or an obvious path toward an intentional breach (leaving the surrounding cortical bone intact). The total depth of the pedicle tracts from the bone surface ranged from 14 mm to 25 mm, as measured with the ruler on pedicle probe. A 1-mm diameter optical fiber was inserted into the bottom of the pre-bored pedicle holes. The optical fiber was used to transmit 750 nm wavelength laser light from a Phocus Mobile laser (Opotek Inc., Carlsbad, CA, USA) with an energy of 13.4 mJ at the fiber tip. An Alpinion SC1-6 convex array ultrasound transducer, which was connected to an Alpinion E-CUBE 12R ultrasound system (Alpinion, Seoul, South Korea), was placed on the exposed tissue surface to receive the photoacoustic signals originating from the tip of the fiber. To assist the surgeon with fiber tip localization, a GPU implementation of SLSC for photoacoustic imaging[17–19] was used during the surgery.

For each fiber tip location, 10 photoacoustic image frames were acquired. SLSC and LW-SLSC beamforming were used to determine the position of the optical fiber tip, which was difficult to determine from DAS

Downloaded From: https://www.spiedigitallibrary.org/conference-proceedings-of-spie on 28 Mar 2021
Terms of Use: https://www.spiedigitallibrary.org/terms-of-use

photoacoustic images due to the presence of incoherent signals that were removed with the coherence-based beamforming.[14,18] Photoacoustic images were overlaid on co-registered ultrasound image acquisitions that were interleaved with photoacoustic image acquisitions. For each photoacoustic acquisition, contour maps were created from the DAS, SLSC, and LW-SLSC photoacoustic images within a 15 mm × 15 mm region surrounding the center of the target identified by LW-SLSC images. The -6, -10, -15, and -20 dB contour lines were displayed in each contour map.

The total area encompassed by each contour line was calculated for each of the four contour levels. A Mann-Whitney test was used to evaluate the statistical significance ($p<0.001$) of the difference in areas measured when the optical fiber was touching either cancellous or cortical bone. The bone type was based on ground truth information available in post-operative CT images. This statistical analysis was repeated for each contour level and for each beamforming method.

3. RESULTS

Fig. 2 shows CT, ultrasound, and overlaid photoacoustic images of an accurately created hole, a lateral breach, and a medial breach, from left to right respectively. The CT slices (top row) were chosen to optimize visual confirmation of the fiber placement description and are not registered to the ultrasound and photoacoustic images. The left CT image shows the tip of the hole surrounded by low density bone (i.e., cancellous bone), where the tip of the optical fiber was placed to generate the corresponding photoacoustic image. The middle and right CT images show the tip of the hole in close proximity to high density bone (i.e., cortical bone). Corresponding photoacoustic signals from the cancellous core and the cortical bone are shown in the bottom row. Qualitatively, the DAS photoacoustic images show a more spatially diffuse pattern when the optical fiber was touching cancellous bone compared to the pattern generated when the fiber was touching cortical bone.

Fig. 3 shows contour plots of the photoacoustic signals originating from cancellous bone (top) and cortical bone (bottom), when zooming in on the regions highlighted by the yellow boxes in Fig. 2. Contour lines are shown after beamforming the associated signals with DAS (left), SLSC (middle), and LW-SLSC (right) beamformers. The diffuse pattern of signals originating from cancellous bone, as observed with DAS beamforming in Fig. 2, complicates localization of the fiber tip. Localization was improved with the use of coherence-based beamforming

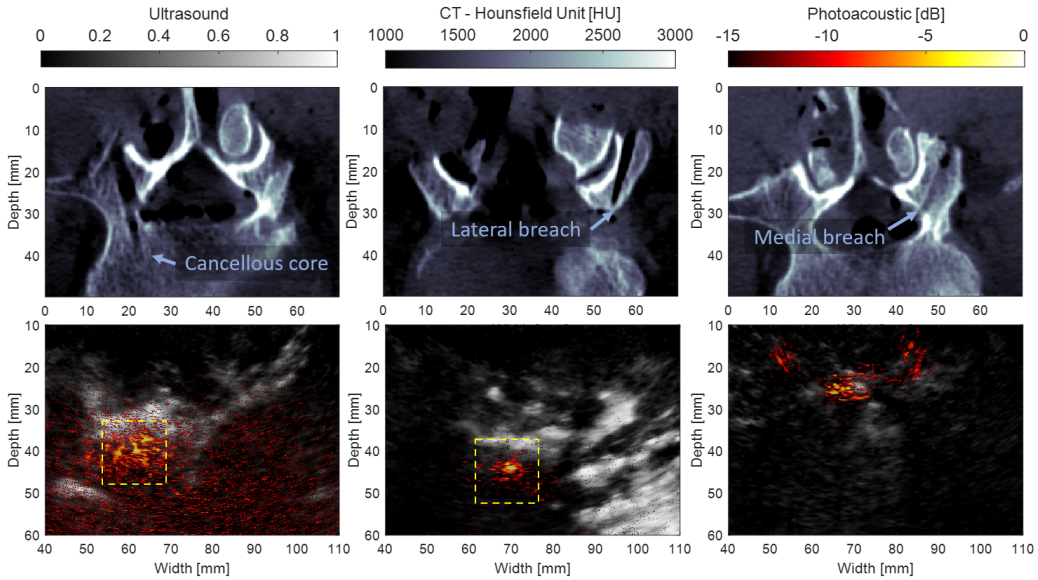

Figure 2: CT axial slice (top) and corresponding LW-SLSC ultrasound images co-registered with DAS photoacoustic image (bottom). The photoacoustic images represent example signals obtained when the tip of the optical fiber touches the bottom of the cancellous core, the cortical bone of a lateral breach, and the cortical bone of a medial breach, from left to right, respectively. The yellow boxes indicate regions of interest for Fig. 3.

Downloaded From: https://www.spiedigitallibrary.org/conference-proceedings-of-spie on 28 Mar 2021
Terms of Use: https://www.spiedigitallibrary.org/terms-of-use

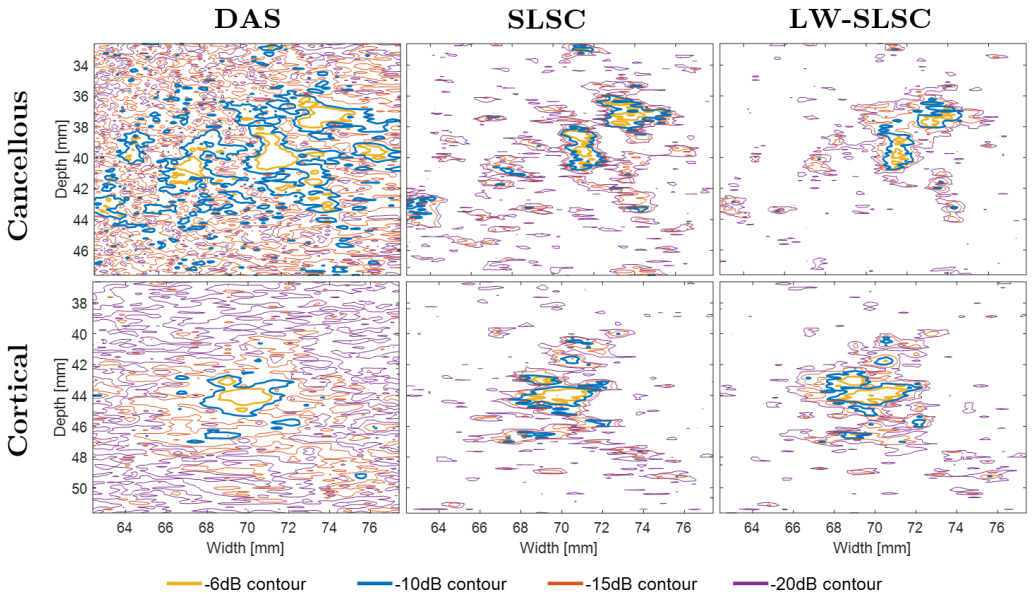

Figure 3: Contour plots of photoacoustic DAS, SLSC, and LW-SLSC images, taken from the region highlighted with the yellow box in Fig. 2, when the tip of the optical fiber was touching cancellous (top) or cortical (bottom) bone.

methods. In particular, the -6 dB and -10 dB contours occupy less total area and are closer together in the corresponding SLSC and LW-SLSC photoacoustic, which enables more accurate localization of the fiber tip. The total areas of the -6 dB contours for the cortical bone were 3.41, 0.40, and 1.06 mm^2 for DAS, SLSC, and LW-SLSC, respectively. In contrast, the total areas of the -6 dB contours for the cancellous bone were 17.55, 0.42, and 0.47 mm^2 for DAS, SLSC, and LW-SLSC, respectively.

Fig. 4 compares the total areas enclosed by the -6, -10, -15, and -20 dB contour levels in DAS, SLSC, and LW-SLSC images, for the cancellous and cortical bone cases shown in Fig. 3, combined with 5 additional cases from an optical fiber in contact with cancellous bone within a prepared pedicle hole and 4 additional cases from

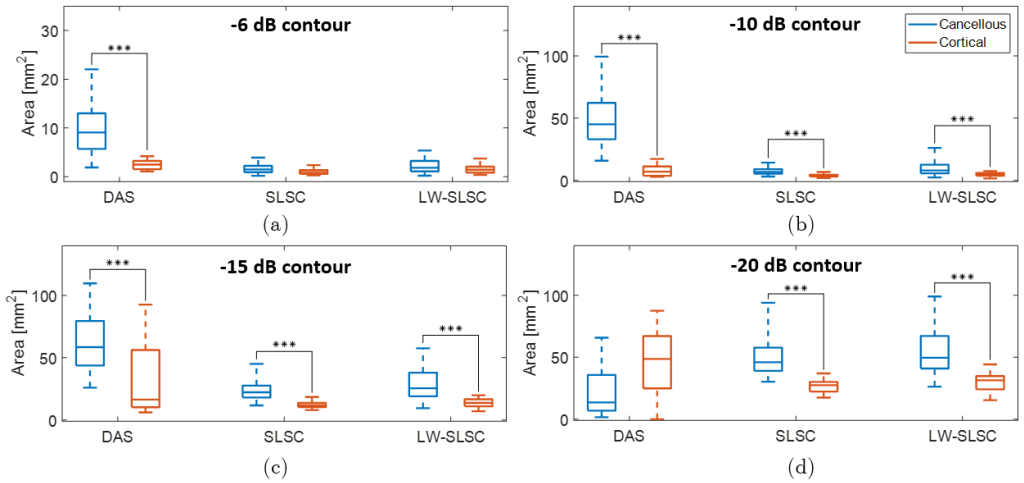

Figure 4: Difference of areas from DAS, SLSC, and LW-SLSC images of photoacoustic targets inside cortical and cancellous bone using contours of (a) -6dB, (b) -10dB, (c) -15dB, and (d) -20 dB. Each boxplot shows the median, interquartile range, maximum and minimum values of the estimated areas over 60 frames for cancellous bone and 50 frames for cortical bone. ***p <0.001.

Downloaded From: https://www.spiedigitallibrary.org/conference-proceedings-of-spie on 28 Mar 2021
Terms of Use: https://www.spiedigitallibrary.org/terms-of-use

an optical fiber in contact with cortical bone after an intentional breach. Each box plot shows the median, interquartile range, maximum, and minimum values of the estimated areas over 60 frames for cancellous and 50 frames for cortical bone (i.e., from 10 repeated acquisitions per case). Overall, DAS, SLSC, and LW-SLSC images showed statistically significant differences between the medians of measured areas from cortical and cancellous bone ($p<0.001$) for contours of -10 dB and -15 dB. In addition, DAS sufficiently differentiated between these two types of bone structures with statistical significance ($p<0.001$) at -6 dB contours. SLSC and LW-SLSC achieved differentiation with statistical significance ($p<0.001$) at -20 dB contour levels, while DAS did not.

4. DISCUSSION

The work presented in this paper is the first to investigate the morphology of photoacoustic signals originating from cancellous and cortical bone within an *ex vivo* human cadaver at multiple contour levels. Previously, we analyzed the feasibility of differentiating photoacoustic signals from cortical and cancellous bone at a contour level of -6 dB, using DAS, SLSC, and LW-SLSC beamforming.[14] This paper presents results for three additional contour levels (i.e., -10, -15, and -20 dB), with the goal of summarizing the relative differentiation capabilities.

While results show that photoacoustic differentiation is possible with either of the three beamformers at contour levels of -10 and -15 dB, using the amplitude-based beamformer (i.e., DAS) and a contour level of -6 dB is considered the most robust solution. The rationale for this robustness is that a contour level of -6 dB allows more localized visualization of the photoacoustic response from the fiber tip (either independently or possibly attached to a surgical tool) without confusing this response from that of surrounding tissue. In addition, differentiation based on the -6 dB contour level is recommended for clinical translation, as out-of-plane signals and photoacoustic reverberations contribute to additive noise that affects higher contour levels, making these higher levels less reliable for differentiation. In contrast, coherence-based photoacoustic imaging enables the localization of fiber tips, which is advantageous in conjunction with anatomical landmarks obtained from ultrasound acquisitions,[14] because surgeons can track the tool tip as the hole is being created in order to ensure a correct trajectory. Accurately created pedicle holes reduce the risk of complications surrounding bone breaches during spinal fusion surgeries. The improved localization of the tool tip can be appreciated by estimating the centroid of the -6 dB contour levels for the SLSC and LW-SLSC images represented in Fig. 3 (in comparison that of the DAS image). Therefore, amplitude- and coherence-based photoacoustic images can be synergistically employed to differentiate between signals originating from cortical and cancellous bone at -6 dB contour levels and to detect the tip of surgical tools, respectively.

In a clinical scenario, the optical fiber can be inserted in the core of the tool used to bore the hole, providing simultaneous DAS-based and SLSC-based photoacoustic images in real-time.[18] A computer vision algorithm could be incorporated into the framework to display in real-time the areas of the -6 dB DAS photoacoustic signals surrounding the fiber tip. When creating the pedicle hole, the area of this contour level would then be expected to decrease if the fiber tip approaches the cortical walls. Therefore, the displayed areas would serve as additional information to the surgeon regarding undesirable proximity to cortical bone, which has the potential to prevent a lateral or medial breach during spinal fusion surgery. In addition to correcting trajectories during the hole creation process, previous work demonstrates that photoacoustic imaging can also be used to determine the appropriate starting point for pedicle cannulation.[12] The combination of these findings with the contributions of this paper constitute a complete photoacoustic-based solution to avoid accidental bone breaches.[14]

5. CONCLUSION

In this paper, we analyzed the morphology of photoacoustic signals originating from cancellous and cortical bone in the pedicles of an *ex vivo* human cadaver, using amplitude-based and coherence-based beamforming techniques. By measuring the area at different contour levels, DAS beamforming provided better photoacoustic differentiation between cancellous and cortical bone in comparison to coherence-based SLSC and LW-SLSC beamforming at the -6 dB contour level. This contour level also enabled both fiber tip localization with the coherence-based beamformers. These results are promising for surgical guidance within the desired cancellous core of the pedicle and away from the surrounding cortical bone, in order to avoid costly and painful bone breaches during spinal fusion surgery.

Downloaded From: https://www.spiedigitallibrary.org/conference-proceedings-of-spie on 28 Mar 2021
Terms of Use: https://www.spiedigitallibrary.org/terms-of-use

Acknowledgments

The authors acknowledge the support of NVIDIA Corporation with the donation of the Titan Xp GPU used for this research. In addition, the authors thank Gerhard Kleinzigand Sebastian Vogt from Siemens Healthineers for making a Siemens ARCADIS Orbic 3D available.

REFERENCES

[1] Manbachi, A., Cobbold, R. S., and Ginsberg, H. J., "Guided pedicle screw insertion: Techniques and training," *The Spine Journal* **14**(1), 165–179 (2014).

[2] Hecht, N., Yassin, H., Czabanka, M., Föhre, B., Arden, K., Liebig, T., and Vajkoczy, P., "Intraoperative computed tomography versus 3D C-arm imaging for navigated spinal instrumentation," *Spine* **43**(5), 370–377 (2018).

[3] Açıkbaş, S., Arslan, F., and Tuncer, M., "The effect of transpedicular screw misplacement on late spinal stability," *Acta Neurochirurgica* **145**(11), 949–955 (2003).

[4] Park, P., Garton, H. J., Gala, V. C., Hoff, J. T., and McGillicuddy, J. E., "Adjacent segment disease after lumbar or lumbosacral fusion: Review of the literature," *Spine* **29**(17), 1938–1944 (2004).

[5] Aota, Y., Kumano, K., and Hirabayashi, S., "Postfusion instability at the adjacent segments after rigid pedicle screw fixation for degenerative lumbar spinal disorders.," *Journal of Spinal Disorders* **8**(6), 464–473 (1995).

[6] Abul-Kasim, K. and Ohlin, A., "The rate of screw misplacement in segmental pedicle screw fixation in adolescent idiopathic scoliosis: The effect of learning and cumulative experience," *Acta Orthopaedica* **82**(1), 50–55 (2011).

[7] Fedrigo, N., "Improving spinal fusions: Redesigning the pedicle probe to prevent vertebral breaches," *Canadian Science Fair Journal* **1**(2) (2019).

[8] Roschger, P., Rinnerthaler, S., Yates, J., Rodan, G., Fratzl, P., and Klaushofer, K., "Alendronate increases degree and uniformity of mineralization in cancellous bone and decreases the porosity in cortical bone of osteoporotic women," *Bone* **29**(2), 185–191 (2001).

[9] Ishak, B., Younsi, A., Wieckhusen, C., Slonczewski, P., Unterberg, A. W., and Kiening, K. L., "Accuracy and revision rate of intraoperative computed tomography point-to-point navigation for lateral mass and pedicle screw placement: 11-year single-center experience in 1054 patients," *Neurosurgical Review* , 1–11 (2018).

[10] Upendra, B. N., Meena, D., Chowdhury, B., Ahmad, A., and Jayaswal, A., "Outcome-based classification for assessment of thoracic pedicular screw placement," *Spine* **33**(4), 384–390 (2008).

[11] Fichtner, J., Hofmann, N., Rienmüller, A., Buchmann, N., Gempt, J., Kirschke, J. S., Ringel, F., Meyer, B., and Ryang, Y.-M., "Revision rate of misplaced pedicle screws of the thoracolumbar spine: Comparison of three-dimensional fluoroscopy navigation with freehand placement: A systematic analysis and review of the literature," *World Neurosurgery* **109**, e24–e32 (2018).

[12] Shubert, J. and Bell, M. A. L., "Photoacoustic imaging of a human vertebra: Implications for guiding spinal fusion surgeries," *Physics in Medicine & Biology* **63**(14), 144001 (2018).

[13] Lediju Bell, M. A., "Photoacoustic imaging for surgical guidance: Principles, applications, and outlook," *Journal of Applied Physics* **128**(6), 060904 (2020).

[14] Gonzalez, E. A., Jain, A., and Bell, M. A. L., "Combined ultrasound and photoacoustic image guidance of spinal pedicle cannulation demonstrated with intact ex vivo specimens," *IEEE Transactions on Biomedical Engineering* (2021).

[15] Lediju, M. A., Trahey, G. E., Byram, B. C., and Dahl, J. J., "Short-lag spatial coherence of backscattered echoes: Imaging characteristics," *IEEE Transactions on Ultrasonics, Ferroelectrics, and Frequency Control* **58**(7), 1377–1388 (2011).

[16] Gonzalez, E. and Bell, M. A. L., "Segmenting bone structures in ultrasound images with locally weighted SLSC (LW-SLSC) beamforming," in [*2018 IEEE International Ultrasonics Symposium (IUS)*], 1–9, IEEE (2018).

Downloaded From: https://www.spiedigitallibrary.org/conference-proceedings-of-spie on 28 Mar 2021
Terms of Use: https://www.spiedigitallibrary.org/terms-of-use

[17] Gonzalez, E. and Bell, M. A. L., "A GPU approach to real-time coherence-based photoacoustic imaging and its application to photoacoustic visual servoing," in [*Photons Plus Ultrasound: Imaging and Sensing 2020*], **11240**, 1124054, International Society for Optics and Photonics (2020).

[18] Gonzalez, E. A. and Bell, M. A. L., "GPU implementation of photoacoustic short-lag spatial coherence imaging for improved image-guided interventions," *Journal of Biomedical Optics* **25**(7), 1 – 19 (2020).

[19] Gonzalez, E., Gubbi, M. R., and Bell, M. A. L., "GPU implementation of coherence-based photoacoustic beamforming for autonomous visual servoing," in [*2019 IEEE International Ultrasonics Symposium (IUS)*], 24–27, IEEE (2019).

Downloaded From: https://www.spiedigitallibrary.org/conference-proceedings-of-spie on 28 Mar 2021
Terms of Use: https://www.spiedigitallibrary.org/terms-of-use